Journal of Superconductivity and Novel Magnetism (2021) 34:2821–2832
https://doi.org/10.1007/s10948-021-06046-y

ORIGINAL PAPER

Comparison of the Dopant Effect and Sample Preparation Method on Y-123 Superconductors

O. Ozturk[1] · A. R. A. Nefrow[1] · F. Bulut[2] · S. Kurnaz[3] · S. Safran[4]

Received: 27 July 2021 / Accepted: 23 September 2021 / Published online: 4 October 2021

Abstract

The detailed comparison of the effects of Co and $CoFe_2O_4$ dopants and preparation methods (solid-state reaction method and sol–gel methods) have been studied on structural, electrical, superconducting, and mechanical properties of Y123 bulk superconductors. The doping amounts of Co and $CoFe_2O_4$ were chosen up to 0.10 wt. %. X-ray powder diffraction (XRD) method, temperature-dependent resistance measurement (*R-T*), and Vickers microhardness analyses were performed to characterize prepared samples. XRD analysis showed that all samples have Pmmm symmetry of orthorhombic crystal structure; intensities and width of the diffraction lines were affected by doping material, but, independent of the preparation method. Although all samples crystallize in orthorhombic structure and exhibit superconductivity behavior, with increasing doping rate the critical transition temperatures of the samples showed a significant decrease and broadened to superconducting temperature transition width. This is more evident in $CoFe_2O_4$-doped Y-123 samples produced by sol–gel method. As the applied force increased, it was observed that the microhardness values of the Co-doped samples increased while the $CoFe_2O_4$-doped samples decreased, regardless of the sample preparation method.

Keywords Y-123 phase · Co and $CoFe_2O_4$ doping · Preparation methods of superconductors

1 Introduction

After the discovery of superconductivity [1], one of the most important enhancements for critical transition temperature of superconductor was appeared in LaBaCuO HTSs (high-temperature superconductors) determined by Bednorz and Muller in 1986 [2]. Following this development, many new oxide type-2 superconductors have been prepared such as BiSrCaCuO, HgBaCaCuO, and YBaCuO with high critical transition temperature over the liquid nitrogen temperature (77 K) [3–5]. The use of liquid nitrogen in applications such as motors, transformers, heavy industry technology, material engineering, and industrial energy provides important advantages such that the implementation is both cheaper and easier than liquid helium. The main goal of these kinds of applications is that high performance and low-cost operation. So that easily accessible and low price of liquid nitrogen is preferable. In this context, many research groups have extensively studied the improvement and examination of main characteristic properties of HTS including the electrical, magnetic, mechanical, crystal structure quality, morphological, crystallinity, couplings, and grain boundary to get high performance. For these purposes, different methods of preparation, pelletization pressures, calcination, and sintering temperatures and durations, stoichiometric ratios, precursor powders with different purity, grinding time, adding, doping, and partial substitution/displacement in the crystal system were applied and these studies were given in the literature [6–13].

There are many different sample preparation methods such as solid-state reaction method, sol–gel method, ammonium nitrate precipitation method, rapid thermal melting process, and microwave processing method in the production of superconductors. The well-known and most used methods are the solid-state reaction (SSR) method and sol–gel

✉ S. Safran
safranserap@gmail.com; safran@science.ankara.edu.tr

[1] Department of Electrical and Electronics Engineering, Kastamonu University, 37100 Kastamonu, Turkey

[2] Scientific and Technological Research Applications and Research Center, Sinop University, 57000 Sinop, Turkey

[3] Central Research Laboratory, Kastamonu University, 37100 Kastamonu, Turkey

[4] Department of Physics, Ankara University, 06100 Ankara, Turkey

(SG) method. In the former method, precursor powders are weighed in stoichiometric proportions, generally mixed in an agate mortar (using by ball-milling machine or by hand), and then annealed at certain high temperatures with proper times to attain the superconducting phases. Carbonate-based compounds and non-reactive metal oxides are generally preferred as starting materials for production of the HTSs [10, 14, 15]. In latter method is a kind of wet chemical route which dissolves one or more metal components in solution [16] and can be a more suitable technique than the former because of easy to achieve chemical homogeneity, control particle size, and morphology [14, 15].

The main superconducting parameters such as critical transition temperature, critical current density, and critical magnetic field can be modified by partial substitution/displacement in the crystal system. Non-magnetic and magnetic materials can be used for this purpose. Non-magnetic dopants can break the coupling and also degrade the lattice arrangement, such as the larger or smaller size of impurities can locate the space inside of the lattice or replace with the main atoms in the structure [17, 18]. The superconducting/ferromagnetic interfaces can be formed by doping magnetic materials into the superconductors. These kinds of magnetic dopants can help to improve the current-carrying capacity of the superconductors utilizing act as a pinning center. On the other hand, a small amount of magnetic dopants can also reduce the flux pinning capacity and deteriorate the transport properties of the superconductors [19]. Improving or destroying the performance of superconductors depends on lots of parameters such as the ratio and size of the dopants, the method of preparation of the sample, the presence of agglomeration, and the interaction between the dopant and superconductor.

We investigated the effect of partial Fe/Cu and Co/Cu replacement on fundamental properties of Y-123 ceramics by substituting $CoFe_2O_4$ and Co [6, 7]. There are also several studies related to $CoFe_2O_4$ and Co substitution to Y-123 ceramics in the literature [20–25]. Our aim is to compare both the effects of $CoFe_2O_4$ and Co dopants and preparation methods on structural, electrical, superconducting, and mechanical properties of Y123 bulk superconductors. We try to define that which magnetic dopant ($CoFe_2O_4$ and Co) and production method (SSR or SG) is much more convenient to prepare the Y-123 ceramic superconductor with higher basic characteristics for new, unique, and applicable market application areas.

2 Experimental Details

In this study, the Cu-site $CoFe_2O_4$ (nano-powder, 30-nm particle size (TEM), 99%, Sigma-Aldrich) and Co (cobalt powder-325 mesh, 99.5%, Alfa Aesar) partial doped $YBa_2Cu_{3-x}O_{7-y}$ superconducting samples (by weight at $x=0$, 0.05, and 0.10) are fabricated by SSR and SG methods. Y_2O_3 (99.99%, Alfa Aesar), $BaCO_3$ (99.95%, Alfa Aesar), and CuO (99.9995%, Alfa Aesar) starting powders were preferred for the production of samples by the SSR method. In the SG method, 15 mL of methanol anhydrous and 15 mL acetic acid were put into the barium acetate powder and stirred up at room temperature until a homogeneous mixture was attained. The homogeneous intermediate mixture was added to yttrium acetate powder and mixed once more. After homogeneity was achieved, copper acetate and the doping elements ($CoFe_2O_4$ and Co) were stirred up the mixture by adding 8 mL of triethanolamine which is used for accelerating the dissolution process of copper. The resulting solution was left in a sealed beaker at room temperature for 12 h, and then the beaker was opened and heated to 80 °C for gelling of the solution. The solution, which reached the consistency of a gel, was applied to heat treatment in the oven at 300 °C for 30 min.

The doping ratio for the structure of $YBa_2Cu_{3-x}O_{7-y}$ was made by weight at $0 \le x \le 0.10$. The precursor powders weighed stoichiometrically and milled in an agate mortar for 1 h using a ball-milling machine. The mixture was placed in an alumina crucible, calcined at 850 °C for 24 h in a tubular furnace three times, and milled between each calcination procedure. The dopants (Co and $CoFe_2O_4$) were added into mixed powders at 0 wt. %, 5 wt. %, and 10 wt. %. The powders were pressed into pellets 10 mm in diameter and 2 mm in thickness under the 200-MPa pressure by using a hydraulic press. The samples were annealed in air at 930 °C for 24 h and then lowered to 500 °C and subjected to oxygen for 5 h. The bulk Co and $CoFe_2O_4$ Y123 superconducting compounds with different doping levels of $x=0.00$, 0.05, and 0.10 will be called with respect to the preparation methods, doping materials, and doping level: SSR-U, SG-U, SSR-C-5, SSR-C-10, SG-C-5, SGR-C-10, SSR-C-5, SSR-CF-10, SG-CF-5, and SG-CF-10, respectively (preparation method (SSR: solid-state reaction method and SG: sol–gel method), doping (U: undoped, C: Co doping, CF: $CoFe_2O_4$ doping), and doping ratio (5 and 10 wt. %)).

XRD measurements were carried out by Bruker D8 Advance diffractometer with CuK_α ($\lambda=1.541$Å) radiation between $2\theta=3°$–90° for scanning speed of 4°/min. The electrical resistivity was measured in Janis CCS-450 by conventional four-probe method for the temperature range of 10–300 K. SHIMADZU HVM-2 microhardness tester was used for microhardness test and measurements were performed at room temperature. An indenter was implemented for 10 s using different load from 0.245 to 2.940 N, and the accuracy of these measurements were ± 0.1 µm. The mechanical measurement was carried out at different locations of sample surfaces with an average of 10 readings to get acceptable values for each load.

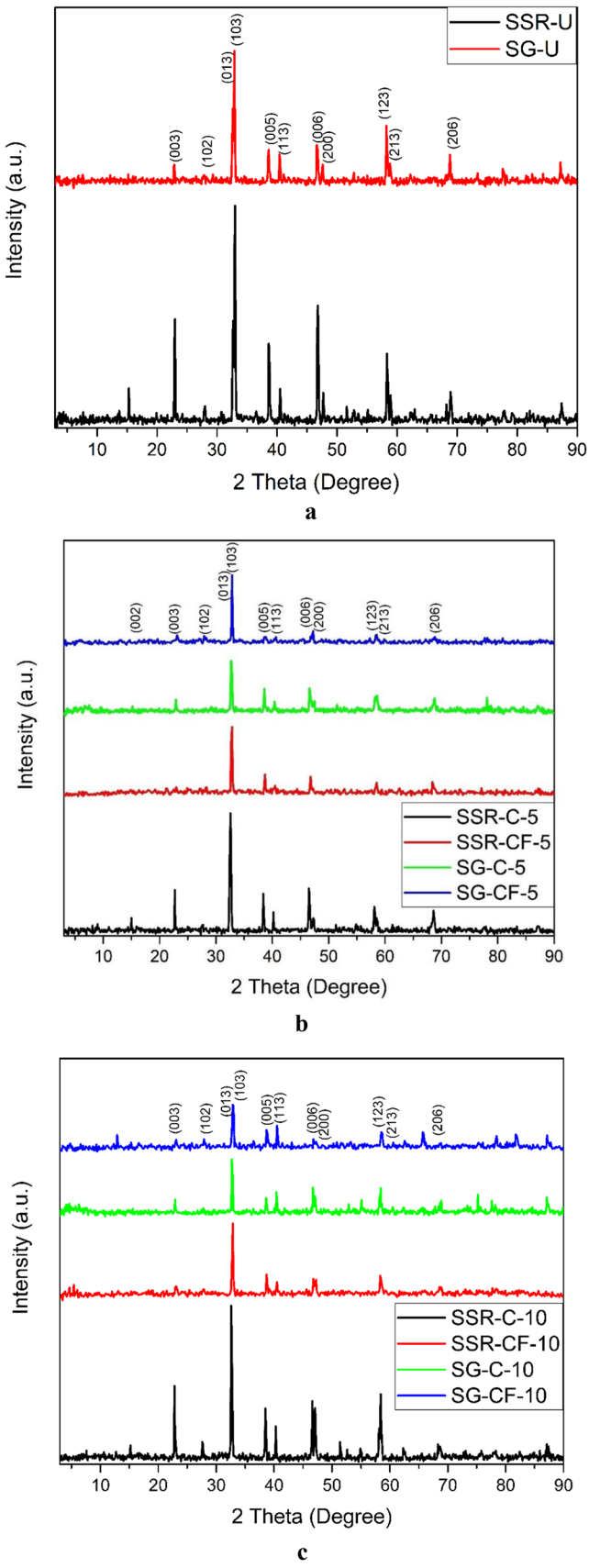

Fig. 1 Comparative XRD graphs for the materials prepared by two different methods: **a** undoped, **b** 5 wt. % doped, and **c** 10 wt. % doped

3 Results and Discussion

3.1 Analysis of XRD Measurements

XRD patterns of undoped, Cu-site Co, and $CoFe_2O_4$ partially doped Y-123 bulk superconductors prepared by SSR and SG methods are shown in Fig. 1a, b. Miller indices of YBCO superconducting phases are displayed in these figures. It indicates that most of the diffraction peaks belong to the orthorhombic structure of Pmmm symmetry for Y-123 superconductor. There is no evidence of the presence of secondary phases in the XRD pattern due to the low doping level. Besides, the intensities of the diffraction lines are going down and also the width of the diffraction lines are narrowing with doping regardless of the doping material and preparation methods. This situation indicates that the crystallization of grains is getting bigger and bigger. One can take information about the approximate crystallite size of the samples from the well-known equation of Scherrer [26]:

$$D = \frac{0.941\ \lambda}{B\ \cos\ \theta} \tag{1}$$

$$B^2 = B_s^2 - B_m^2 \tag{2}$$

Here D, θ, λ, and B_s represent average crystallite size, Bragg angle, the wavelength of the incident X-ray beam, and the full width half maximum (FWHM) value for the (103) diffraction line, respectively, and $B_m = 0.000007$ [27]. The lattice parameters (a, b, and c) of the orthorhombic structure determined from XRD data are calculated using the distance between the planes (d) and (hkl) Miller indices of the plane:

$$\frac{1}{d^2} = \frac{h^2}{a^2} + \frac{k^2}{b^2} + \frac{l^2}{c^2} \tag{3}$$

The calculated Scherrer average crystallite size and orthorhombicity value ($\delta = 100(a-b)/(a+b)$) and lattice parameters are given in Table 1 and Fig. 2a, b respectively. The influence of Fe on the grain size refinement of sintered YBCO has been also studied in [28]. As stated earlier in the text, the samples are Y-123 superconductors with orthorhombic structures. However, the crystal structure of Y-123 can be tetragonal or orthorhombic depending on the stoichiometry. YBCO has superconducting properties when crystallized in an orthorhombic structure, but when crystallized in a tetragonal structure, it does not behave like a superconductor but acts as an insulator. The lack of oxygen and/or doping in the stoichiometry may cause the sample that needs to crystallize in orthorhombic structure to approach tetragonal structure. In determining whether the crystal structure of YBCO is closer to the tetragonal structure or orthorhombic structure, it can be interpreted by analyzing the orthorhombicity value, lattice parameters, and diffraction peaks of XRD patterns. It can be said that when the orthorhombic value decreases and approaches zero and/or when the lattice parameters a and b close to each other, the structure shifts to the tetragonal structure and does not show any superconducting properties (T_c, J_c, H_c). A comparison of the δ values given in Table 1 shows that undoped samples prepared by SG method may have better superconducting properties than SSR method. However, when doping is performed, the sample produced by the SSR method appears to have greater δ values, regardless of the doping material. A systematic behavior between doping materials (Co and $CoFe_2O_4$) and δ values could not be determined. But δ values of doped samples prepared by the SSR method are higher than the SG method. This is also compatible with lattice parameters. The lattice parameters, a and b, getting closer with doping but this approach is much more for the SG method (Fig. 2). It can be interpreted that SSR samples may have better superconducting properties than SG samples because of orthorhombicity value. In addition, the lattice parameters (a, b, and c) calculated for the SSR method are consistent with the literature. Although the lattice parameters for the SG method do not exactly match it [10]. The lattice parameters are changed very slightly with doping. This is due to the amount of doping being as small as 5 wt. % and 10 wt. %. But, some amount of doping material (Co and $CoFe_2O_4$) can partly replace or substitute by Cu^{+2} ions. This is possible because the ionic radius of Cu^{+2} (0.730 Å) is comparable with the ionic radii of Co^{3+} (0.745 Å) and Cu^{+2} ions replaced by Co^{3+} ions caused some changes in the crystal lattice parameters, but did not disturb the crystal structure. Besides, Fe^{2+} ions (0.820 Å) having a larger radius than Cu ions caused more changes in $CoFe_2O_4$-doped samples compared to Co-doped samples.

Table 1 Crystallite size and orthorhombicity parameters for undoped and $CoFe_2O_4$ and Co-doped Y-123 ceramic superconductors

Sample	D (nm)	δ (orthorhombicity)
SSR-U	28.95	0.78
SG-U	28.21	1.04
SSR-C-5	*29.53*	*0.78*
SSR-CF-5	*30.16*	*0.65*
SG-C-5	*31.59*	*0.13*
SG-CF-5	*30.27*	*0.26*
SSR-C-10	37.63	0.78
SSR-CF-10	30.78	0.78
SG-C-10	32.90	0.26
SG-CF-10	29.25	0.39

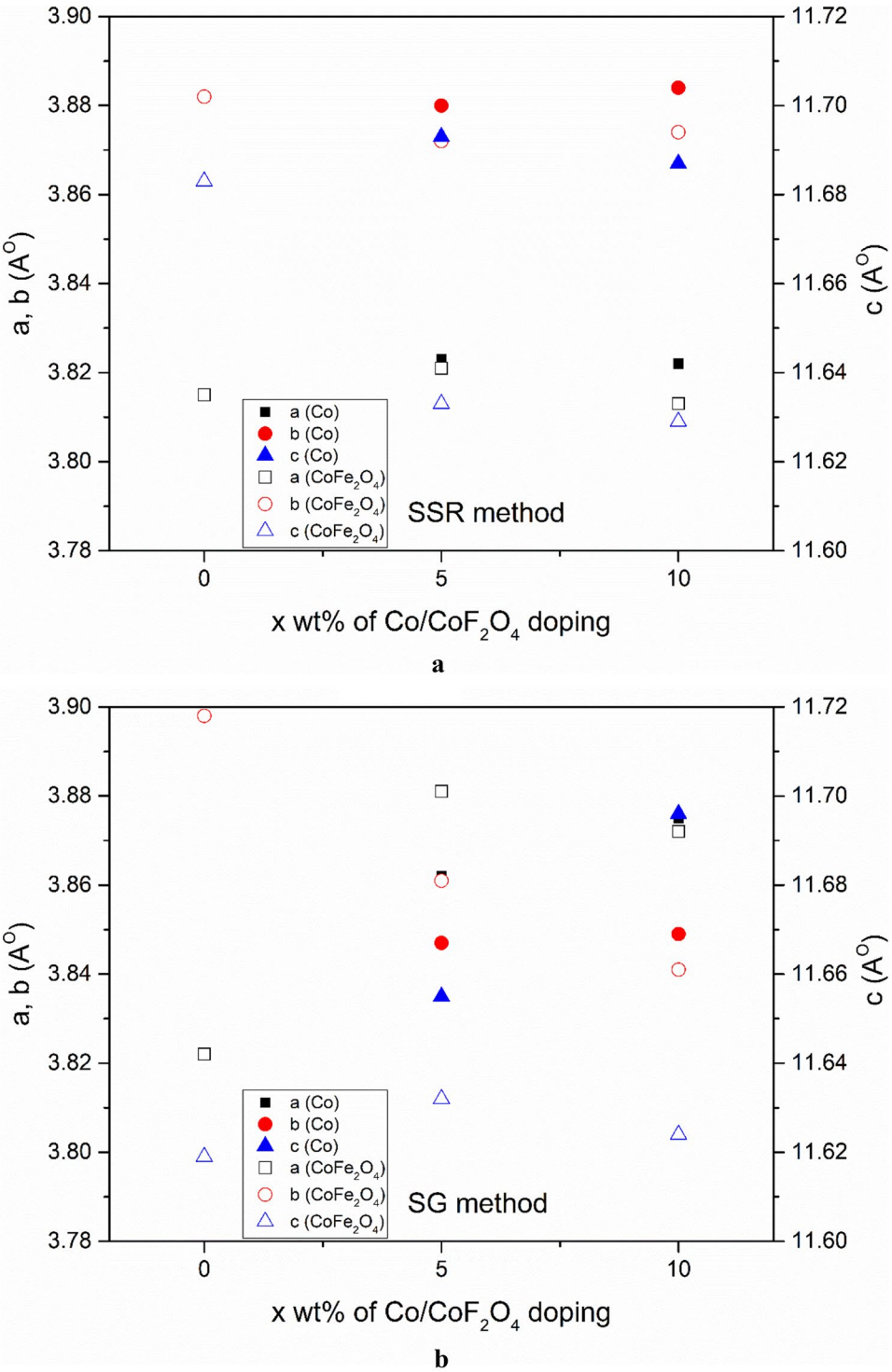

Fig. 2 Lattice parameters versus wt. % $Co/CoFe_2O_4$ doping ratio graph prepared by **a** solid-state reaction methods and **b** sol–gel method

3.2 Analysis of Electrical Resistance Measurement

To determine the critical transition temperature of undoped and Cu-site Co and $CoFe_2O_4$ partially doped Y-123 bulk superconductors prepared by SSR and SG methods, we have measured resistance versus temperature dependence between 40 and 100 K as shown in Fig. 3a, b. The onset critical transition temperature at which superconductivity begins to occur and offset critical transition temperature at which the sample is fully superconducting are given as T_C^{onset} andT_C^{offset}, respectively.T_C^{onset},T_C^{offset}, and the superconducting temperature transition width (ΔT_c) of samples are given in

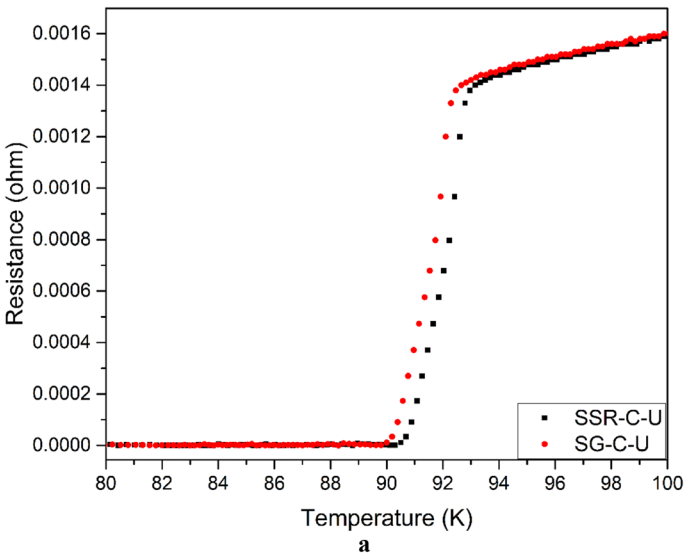

Fig. 3 Comparative temperature-dependent electrical resistance measurements of materials prepared by two different methods: **a** undoped, **b** 5 wt. % doped, and **c** 10 wt. % doped

Table 2. ΔT_c or the sharpness in transition to superconductivity on the graph of *R-T* give information about the capacity of the weak link. A sharper transition or a smaller ΔT_c implies a strong intergranular connection. When doping is applied, ΔT_c values increase from 2.7 K to 16.7 K in the SSR method; this increment is bigger from 2.5 K to 21.5 K in SG method. The samples prepared by SSR method have sharper superconducting transition than samples prepared by SG method. Independent of the preparation method, the behavior of room temperature resistance,T_C^{onset}, T_C^{offset}, and ΔT_c values of undoped samples are almost the same. As can be seen from Fig. 3a and Table 2, undoped samples have higher T_c values and narrower ΔT_c than Co and $CoFe_2O_4$ partially doped Y-123 bulk superconductors. T_C^{onset}andT_C^{offset} values tend to decrease and ΔT_c values are getting bigger with Co and $CoFe_2O_4$ addition. Additionally, compared the ΔT_c values of the doped samples, it was determined that the ΔT_c values of the $CoFe_2O_4$ doped samples in the SSR method are lower than SG method. The same situation is true for cobalt-doped samples. Co and Fe ions may partially replace with Cu ions or the same impurities because doping can settle in the space between the grains in the Y-123 matrix. The presence of these impurities affects the fundamental superconducting properties. The deterioration of critical temperature values can be the sign that Co and Fe ions penetrate the YBCO crystal structure. This may disrupt electron–phonon-electron coupling and these imperfections decrease the mean free path of the electrons, increasing the depth of penetration and decreasing the coherence length. The widening of ΔT_c and decrement of T_C^{offset} is more remarkable for $CoFe_2O_4$-doped Y-123 bulk superconductors than Co-doped samples. Although we do not see any diffraction peaks of impurities and/or secondary phases in the XRD graphs because of small doping ratios, the study of Wimbush et al. [29] showed that the addition of $CoFe_2O_4$ negatively affects the formation of the Y-123 phase. Y(Fe, Co)O_3 phase is formed in $CoFe_2O_4$-doped Y-123 samples. This secondary phase causes yttrium deficiency and disrupts the superconducting properties.

All samples show metal-like behavior over the critical transition temperature. The doped samples appear to have higher resistance in the normal state, while the behavior of room temperature resistance of undoped samples is almost the same as independent of the preparation method. Impurities entering the structure by doping, partial displacements of Co/Cu and/or Fe/Cu in the Y-123 matrix, porosity, presence of secondary phases, and grain boundary coupling problems also may increase the normal state resistance by reducing the average free path of electrons. It can be stated here that $CoFe_2O_4$-doped Y-123 samples have lower T_C^{offset} values and lower room temperature resistance comparing with Co-doped Y-123 samples except for SSR-C-5. These results are compatible with the XRD measurements.

3.3 Analysis of Microhardness Measurement

Microhardness measurements are generally applied with microprobe to determine the mechanical response of materials. The analysis of the mechanical features of superconducting samples is very crucial for the potential usage in application fields, i.e., energy technology, the industrial, potential metallurgical, and materials science engineering of superconductors [30]. The fracture toughness, elastic modulus, stiffness, impact resistance, yield strength, mechanical durability, brittleness index parameters, etc. are determined by mechanical measurements. In this respect, Vickers hardness, Knoop, Rockwell, and Brinell tests are applied [31, 32]. Among these methods, the most common way to determine the mechanical properties of superconducting materials is Vickers hardness measurement because of low cost, fast, simple, reliable, non-destructive, small indentation trace, etc. [33, 34]. Vickers hardness measurements are taken by an indenter with the contact of the sample surface applying a proper load and time. The hardness values of samples are calculated by applying five different loads to the sample surface for 10 s. A diamond-like shape is formed on the sample surface after the applied load is removed. The area of the diamond-like shape is calculated by the measurement of the diagonals of this shape. The Vickers hardness (H_v) parameters are determined by

$$H_V = 1854.4\left(\frac{F}{d^2}\right) \tag{4}$$

Here $d^2 = (\frac{d_1+d_2}{2})^2$ is the area of indentation by measured diagonal length and F is the applied external load on the sample surface. The yield strength (Y), elastic modulus (E), and fracture toughness (K_{IC}) parameters of samples are also

Table 2 The critical transition temperature and superconducting transition temperature interval for all prepared Y-123 samples deduced from temperature-dependent electrical resistance measurements

Sample	Critical Transition temperature (K)		ΔT_C(K)
	T_C^{onset}	T_C^{offset}	T_C^{onset}-T_C^{offset}
SSR-U	93.0	90.3	2.7
SG-U	92.5	90.0	2.5
SSR-C-5	*92.8*	*87.9*	*4.9*
SSR-CF-5	*89.5*	*83.2*	*6.3*
SG-C-5	*89.1*	*79.4*	*9.7*
SG-CF-5	*81.9*	*73.9*	*8.0*
SSR-C-10	92.6	76.7	15.9
SSR-CF-10	89.3	72.6	16.7
SG-C-10	89.1	72.7	16.4
SG-CF-10	89.1	67.6	21.5

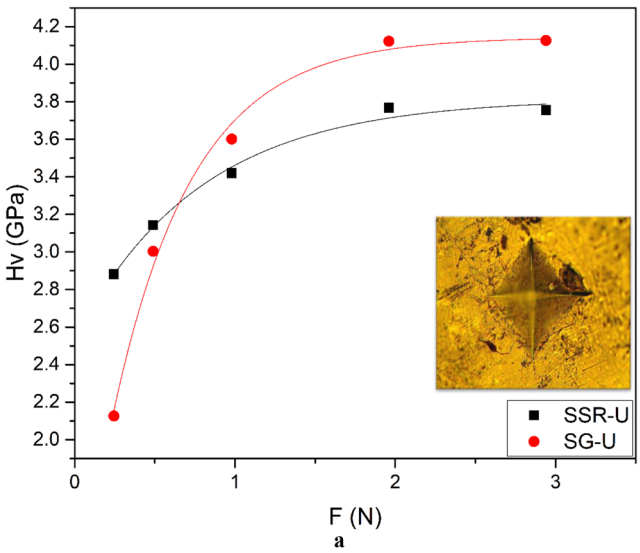

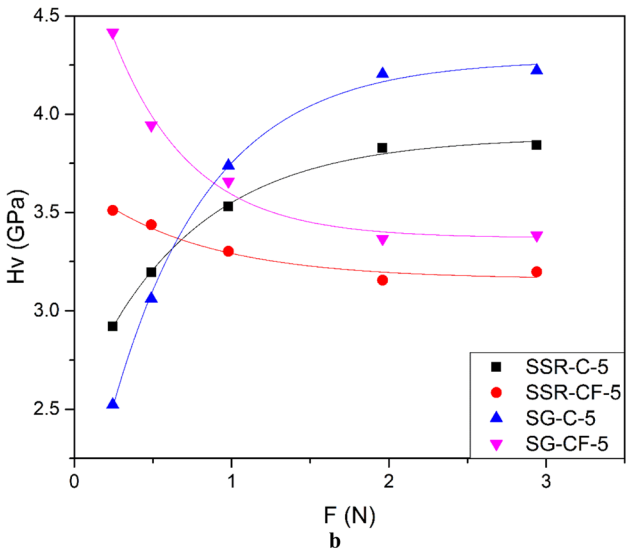

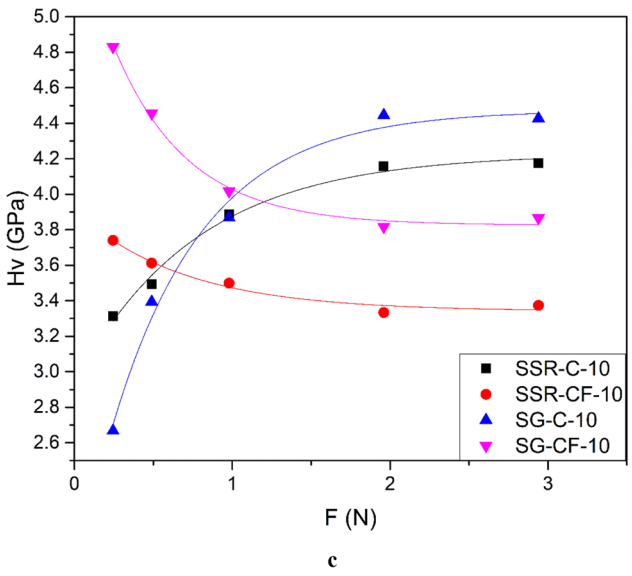

Fig. 4 Comparative Vickers hardness parameters for samples prepared by two different methods: **a** undoped, **b** 5 wt. % doped, and **c** 10 wt. % doped

determined by using H_V values from the following formulas [32]:

$$Y \approx H_V/3 \tag{5}$$

$$E = 81.9635\, H_V \tag{6}$$

$$K_{IC} = \sqrt{2E\gamma} \tag{7}$$

Here γ is the surface energy of the cracks in the sample during the application of the load. The γ value is obtained from $(F/d) - d$ graph and it is the value where axis intersected of the line. The value of α is negative for all samples. Negative α values confirm that the character of the displacement of these materials is in the form of the *RISE* behavior. Negative value relates only to material behavior. It is not a mathematical expression. This situation confirms that the plastic deformations occur in these samples which show the *RISE* behavior. For example, the *F/dd* graph of the SSR-U and SG-U samples is as follows. The γ values obtained are − 0.00979 and − 0.0232. Fracture toughness (K_{IC}) values are calculated using these γ and elastic modulus (E) values. The calculated Vickers microhardness values versus an applied external load of undoped, 5 wt. % and 10 wt. %. $CoFe_2O_4$ and Co partially doped samples depending on preparation methods are graphically shown in Fig. 4a–c, respectively. H_V, Y, E, and K_{IC} parameters depending on applied are external load are given in Table 3 in detail. There are two types of behavior generally observed in the $H_V - F$ graphs. In the former, the H_V values increase as the applied forces increase, while in the other, it is seen that the H_V values decrease as the applied forces increase. These behaviors are called Reverse Indentation Size Effect (RISE) and Indentation Size Effect (ISE), respectively [35, 36]. The undoped samples, SG-U and SSR-U (prepared by either the SG or SSR techniques), show RISE behavior. However, $CoFe_2O_4$-doped samples exhibit ISE while Co-doped samples have RISE behavior independent of the preparation method. Although RISE behavior has been observed in various examples, the reason is still not fully explained. There are different approaches in the literature. It is stated that metallic specimens can harden during loading (when force is applied) and that some cracks may occur in the brittle specimens during the loading of the indentation. According to Feltham and Banerjee, this behavior is related to energy loss due to some disintegration around the indentation [37]. Higher microhardness values can be obtained by applying a load during the indentation process, as the cracks in the sample cause smaller size formation. The formation of cracks in the sample during indentation causes the elastic deformation energy to be released. This reduces the resistance to sample indentation. As a result, it increases the hardness values. Among the

Table 3 H_V, E, and Y values for every material at different applied test loads

Sample	F (N)	H_V (GPa)	E (GPa)	Y (GPa)	K_{IC} (Pa/m$^{1/2}$)
SSR-U	0.245	2.881	236.15	0.960	− 2.151
	0.490	3.143	257.63	1.048	− 2.247
	0.980	3.420	280.28	1.140	− 2.343
	1.960	3.768	308.80	1.256	− 2.460
	2.940	3.755	307.80	1.252	− 2.456
SG-U	*0.245*	*2.126*	*174.25*	*0.709*	*− 2.849*
	0.490	*3.073*	*251.87*	*1.024*	*− 3.425*
	0.980	*3.601*	*295.15*	*1.200*	*− 3.708*
	1.960	*4.122*	*337.85*	*1.374*	*− 3.967*
	2.940	*4.126*	*338.18*	*1.375*	*− 3.969*
SSR-C-5	0.245	2.922	239.47	0.974	− 2.166
	0.490	3.195	261.87	1.065	− 2.265
	0.980	3.530	289.31	1.177	− 2.381
	1.960	3.828	313.75	1.276	− 2.479
	2.940	3.841	314.84	1.280	− 2.484
SSR-CF-5	*0.245*	*3.510*	*287.712*	*1.170*	*2.374*
	0.490	*3.437*	*281.695*	*1.146*	*2.349*
	0.980	*3.302*	*270.670*	*1.101*	*2.303*
	1.960	*3.155*	*258.617*	*1.052*	*2.251*
	2.940	*3.198*	*262.109*	*1.066*	*2.266*
SG-C-5	0.245	2.523	206.77	0.841	− 3.103
	0.490	3.031	248.45	1.010	− 3.402
	0.980	3.638	298.16	1.213	− 3.727
	1.960	4.204	344.59	1.401	− 4.006
	2.940	4.221	345.93	1.407	− 4.014
SG-CF-5	*0.245*	*4.415*	*361.883*	*1.472*	*4.106*
	0.490	*3.943*	*323.204*	*1.314*	*3.880*
	0.980	*3.658*	*299.799*	*1.219*	*3.737*
	1.960	*3.366*	*275.896*	*1.122*	*3.585*
	2.940	*3.384*	*277.343*	*1.128*	*3.594*
SSR-C-10	0.245	3.313	271.51	1.104	− 2.306
	0.490	3.492	286.23	1.164	− 2.368
	0.980	3.887	318.59	1.296	− 2.498
	1.960	4.157	340.73	1.386	− 2.584
	2.940	4.175	342.20	1.392	− 2.589
SSR-CF-10	*0.245*	*3.740*	*306.553*	*1.247*	*2.451*
	0.490	*3.612*	*296.083*	*1.204*	*2.408*
	0.980	*3.499*	*286.788*	*1.166*	*2.370*
	1.960	*3.334*	*273.228*	*1.111*	*2.314*
	2.940	*3.374*	*276.515*	*1.125*	*2.327*
SG-C-10	0.245	2.668	218.66	0.889	− 3.191
	0.490	3.394	278.19	1.131	− 3.600
	0.980	3.868	317.02	1.289	− 3.843
	1.960	4.445	364.37	1.482	− 4.120
	2.940	4.427	362.88	1.476	− 4.111

Table 3 (continued)

Sample	F (N)	H_V (GPa)	E (GPa)	Y (GPa)	K_{IC} (Pa/m$^{1/2}$)
SG-CF-10	*0.245*	*4.829*	*395.815*	*1.610*	*4.294*
	0.490	*4.456*	*365.228*	*1.485*	*4.124*
	0.980	*4.017*	*329.242*	*1.339*	*3.916*
	1.960	*3.817*	*312.815*	*1.272*	*3.817*
	2.940	*3.867*	*316.921*	*1.289*	*3.842*

samples produced in our study, the microhardness values of all samples displaying RISE behavior were higher. H_V values with respect to rising applied load tend to decrease with particular $CoFe_2O_4$ dopant level and reached to plateau region over 2-N applied load. It means that the surface layer of the sample is affected at small applied loads and the surface response is very strong. However, as the load applied to the sample surface increases, the depth of the trace formed on the surface increases, so the reaction of the inner layers becomes more evident. After a while with increasing load, a saturation of hardness is reached.

It is observed that the microhardness value decreased as the applied load increased but increased with rising $CoFe_2O_4$ doping from 5 wt. % to 10 wt. %. The increase in the microhardness value of the materials with the dopant level can be associated with the reduction of the particle size and the increment of the porosity between the particles. In addition, it can be concluded that the samples produced by the SG route have far higher H_V values than in comparison to all materials fabricated by the SSR technique independent of the doping materials and doping level.

As seen in Table 3, E and Y values change depending on the applied load and the doping material. These values rise with increasing Co-contribution and applied load. However, these reduce as the contribution of $CoFe_2O_4$ and the applied load increased. An increase in porosity, reduction in grain size, cracks, and decrease in microhardness may cause this situation. γ is obtained from the point where the $F/d - d$ graph intersects the y axis. While γ values of materials exhibiting ISE behavior are positive, the values of samples exhibiting RISE behavior are negative. In materials exhibiting RISE behavior, plastic deformation is observed, while elastic deformation is not observed or does not occur to the extent comparable to plastic deformation. The formation of plastic deformation means that when the load applied to the material is removed, there is no recycling and the formation of surface cracks. The change in value K_{IC} corresponds to the change in the energy of the average surface cracks. In addition, it is not a mathematical case that this value is negative. It is only related to obtaining negative values of samples exhibiting RISE behavior. In other words, negative K_{IC} means that the mechanical behavior of the material is RISE.

4 Conclusion

In this study, the structural, superconducting, and mechanical properties of the Co- and $CoFe_2O_4$-doped Y123 structure produced by solid-state reaction and sol–gel methods were examined and the obtained data were interpreted with various comparisons. Findings discussed throughout the study are summarized below:

- The doping process caused a change in the diffraction line intensities and a narrowing occurred in the width of the diffraction line regardless of the doping material and preparation methods from the XRD results.
- We can conclude that $CoFe_2O_4$ doping more adversely affected the structural properties than Co doping and the SSR method is also a more convenient preparation method than the SG method for structural properties of Y-123 bulk superconductors.
- As a result of the resistance values taken depending on the temperature to determine the critical temperature value of the superconductor samples, it is seen that the increase in the doping ratio decreases the critical temperature value. This is true for both methods and dopant materials. It is clearly seen that the samples prepared by the SSR method are less affected by the doping process on the critical temperature values compared to the samples prepared by the SG method.
- The hardness values of the samples produced by the SSR method were lower than the samples produced with SG method. In addition, the hardness values of the Co added samples are higher than the $CoFe_2O_4$-doped samples in the plateau region.
- The hardness behavior of the Co-doped samples was RISE as in the samples without doping. In the $CoFe_2O_4$-doped samples, the hardness value increased with the doping, but it was lower than the undoped sample. In addition, the $CoFe_2O_4$-doped samples exhibited ISE behavior different from the undoped sample.

References

1. Onnes, H.K.: Further Experiments with Liquid Helium. D. On the change of the electrical resistance of pure metals at very low temperatures, etc. V. The Disappearance of the resistance of mercury, in: K. Gavroglu, Y. Goudaroulis (Eds.), Through Meas. to Knowl. Sel. Pap. Heike Kamerlingh Onnes 1853–1926, Springer Netherlands, Dordrecht. 264–266 (1991). https://doi.org/10.1007/978-94-009-2079-8_16
2. Müller, J.G.B.A.: Possible high T_c superconductivity in the Ba–La–Cu–O system. Z. Phys. B - Condens. Matter. **64**, 189–193 (1986). https://doi.org/10.1007/BF01303701
3. Harabor, A., Rotaru, P., Harabor, N.A., Nozar, P., Rotaru, A.: Orthorhombic YBCO-123 ceramic oxide superconductor:

structural, resistive and thermal properties. Ceram. Int. **45**, 2899–2907 (2019). https://doi.org/10.1016/j.ceramint.2018.07.272
4. Aliabadi, A., Akhavan Farshchi, Y., Akhavan, M.: A new Y-based HTSC with T_c above 100 K. Phys. C Supercond. Its Appl. **469**, 2012–2014 (2009). https://doi.org/10.1016/j.physc.2009.09.003
5. Guner, S.B., Zalaoglu, Y., Turgay, T., Ozyurt, O., Ulgen, A.T., Dogruer, M., Yildirim, G.: A detailed research for determination of Bi/Ga partial substitution effect in Bi-2212 superconducting matrix on crucial characteristic features. J. Alloys Compd. **772**, 388–398 (2019). https://doi.org/10.1016/j.jallcom.2018.09.071
6. Ozturk, O., Nefrow, A.R.A., Bulut, F., Ada, H., Turkoz, M.B., Yildirim, G.: Effect of Co/Cu partial replacement on fundamental features of Y-123 ceramics. J. Mater. Sci. Mater. Electron. **31**, 7630–7641 (2020). https://doi.org/10.1007/s10854-020-03281-2
7. Safran, S., Bulut, F., Nefrow, A.R.A., Ada, H., Ozturk, O.: Characterization of the $CoFe_2O_4$/Cu displacement effect in the Y123 superconductor matrix on critical properties. J. Mater. Sci. Mater. Electron. (2020). https://doi.org/10.1007/s10854-020-04578-y
8. Slimani, Y., Hannachi, E., Ekicibil, A., Almessiere, M.A., Ben Azzouz, F.: Investigation of the impact of nano-sized wires and particles TiO_2 on Y-123 superconductor performance. J. Alloys Compd. **781**, 664–673 (2019). https://doi.org/10.1016/j.jallcom.2018.12.062
9. Jasim, S.E., Jusoh, M.A., Hafiz, M., Jose, R.: Fabrication of superconducting YBCO nanoparticles by electrospinning. Procedia Eng. **148**, 243–248 (2016). https://doi.org/10.1016/j.proeng.2016.06.595
10. Yeoh, L.M., Ahmad, M.: Characterization and synthesis of Y0.9Ca0.1Ba1.8Sr0.2Cu3O7-δvia combining sol-gel and solid-state route. J. Non. Cryst. Solids. **354**, 4012–4018 (2008). https://doi.org/10.1016/j.jnoncrysol.2008.04.008
11. Ulgen, A.T., Turgay, T., Terzioglu, C., Yildirim, G., Oz, M.: Role of Bi/Tm substitution in Bi-2212 system on crystal structure quality, pair wave function and polaronic states. J. Alloys Compd. **764**, 755–766 (2018). https://doi.org/10.1016/j.jallcom.2018.06.142
12. Öztürk, H., Safran, S.: Effects of carbon-encapsulated nano boron addition on superconducting parameters of BSCCO. J. Alloys Compd. **731**, 831–838 (2018). https://doi.org/10.1016/j.jallcom.2017.10.095
13. Safran, S.: Critical current density and mechanical performance of MgB2 superconductors prepared with different magnesium sources. Ceram. Int. **45**, 10243–10249 (2019). https://doi.org/10.1016/j.ceramint.2019.02.077
14. Matskevich, N.I., Wolf, T.: Thermochemical investigation of YBa2Cu3O7−δ superconductor doped by lutetium. J. Alloys Compd. **614**, 415–419 (2014). https://doi.org/10.1016/j.jallcom.2014.06.125
15. Yilmaz, M., Dogan, O.: Structural and superconducting properties in Y0.6Gd0.4Ba2(Nb)Cu3O7−y cuprates doped with niobium. J. Rare Earths. **30**, 241–244 (2012). https://doi.org/10.1016/S1002-0721(12)60031-3.
16. Klemkiene, T., Raudonis, R., Beganskiene, A., Zalga, A., Grigoraviciute, I., Kareiva, A.: Scandium and gallium substitution effects in the (Y1−xScx)Ba2Cu4O8 and (Y1−xGax)Ba2Cu4O8 superconducting oxides. Mater. Chem. Phys. **119**, 208–213 (2010). https://doi.org/10.1016/j.matchemphys.2009.08.059
17. Alloul, H., Bobroff, J., Mendels, P.: Comment on "Al NMR local probe of local moments induced by an Al impurity in high-T_c cuprate La1.85Sr0.15CuO4". Phys. Rev. Lett. **78**, 2494–2494 (1997). https://doi.org/10.1103/PhysRevLett.78.2494
18. Zhou, Y.X., Scruggs, S., Salama, K.: Effects of ionic doping on superconducting properties of melt textured YBa2($Cu_{1-x}M_x$)3O7-y(M = Co, Ni, Zn or Ga) large grains. Supercond. Sci. Technol. **19**, S556–S561 (2006). https://doi.org/10.1088/0953-2048/19/7/s26
19. Bouchoucha, I., Ben Azzouz, F., Annabi, M., Zouaoui, M., Ben Salem, M.: The study on the ZnO and Zn0.95Mn0.05O added YBCO system: investigation of microstructure and transport properties. Phys. C Supercond. **470**, 262–268 (2010). https://doi.org/10.1016/j.physc.2009.11.034
20. Slimani, Y., Hannachi, E., Ben Salem, M.K., Hamrita, A., Ben Salem, M., Ben Azzouz, F.: Excess conductivity study in nano-$CoFe_2O_4$-added $YBa_2Cu_3O_{7-d}$ and $Y_3Ba_5Cu_8O_{18\pm x}$ superconductors. J. Supercond. Nov. Magn. **28**, 3001–3010 (2015). https://doi.org/10.1007/s10948-015-3144-0
21. Slimani, Y., Hannachi, E., Ben Salem, M.K., Hamrita, A., Varilci, A., Dachraoui, W., Ben Salem, M., Ben Azzouz, F.: Comparative study of nano-sized particles $CoFe_2O_4$ effects on superconducting properties of Y-123 and Y-358. Phys. B Condens. Matter. **450**, 7–15 (2014). https://doi.org/10.1016/j.physb.2014.06.003
22. Sahoo, B., Routray, K.L., Panda, B., Samal, D., Behera, D.: Excess conductivity and magnetization of CoFe2O4 combined with Y1Ba2Cu3O7-δ as a superconductor. J. Phys. Chem. Solids. **132**, 187–196 (2019). https://doi.org/10.1016/j.jpcs.2019.04.035
23. Slimani, Y., Hannachi, E., Ben Azzouz, F., Ben Salem, M.: Comparative study of the effect of magnetic nanoparticle $CoFe_2O_4$ on fluctuation-induced conductivity of Y-123 and Y-358 superconductors. J. Supercond. Nov. Magn. **32**, 511–519 (2019). https://doi.org/10.1007/s10948-018-4746-0
24. Elizabeth, S., Anand, A., Bhat, S.V., Subramanyam, S.V., Bhat, H.L.: Influence of cobalt doping on superconducting transition in as-grown YBCO single crystals. Solid State Commun. **109**, 333–338 (1999). https://doi.org/10.1016/S0038-1098(98)00553-5
25. Wang, W.T., Pu, M.H., Lei, M., Zhang, H., Wang, Z., Zhang, H., Cheng, C.H., Zhao, Y.: Enhanced flux pinning properties in superconducting YBa2Cu3O7−z films by a novel chemical doping approach. Phys. C Supercond. **493**, 104–108 (2013). https://doi.org/10.1016/j.physc.2013.03.039
26. Ahmadipour, M., Ain, M.F., Ahmad, Z.A.: Effects of annealing temperature on the structural, morphology, optical properties and resistivity of sputtered CCTO thin film. J. Mater. Sci. Mater. Electron. **28**, 12458–12466 (2017). https://doi.org/10.1007/s10854-017-7067-3
27. Terzioglu, C., Yilmazlar, M., Ozturk, O., Yanmaz, E.: Structural and physical properties of Sm-doped Bi1.6Pb0.4Sr2Ca2−xSmxCu3Oy superconductors, Phys. C Supercond. Its Appl. **423**, 119–126 (2005). https://doi.org/10.1016/j.physc.2005.04.008
28. Diko, P., Duvigneaud, P.H., Lanckbeen, A., Van Moer, A., Naessens, G., Deltour, R.: Influence of iron doping on the microstructure of $YBa_2(Cu_{1-x}Fe_x)O_{7-y}$ ceramics. J. Am. Ceram. Soc. **76**, 2856–2864 (1993). https://doi.org/10.1111/j.1151-2916.1993.tb04027.x
29. Wimbush, S.C., Yu, R., Bali, R., Durrell, J.H., MacManus-Driscoll, J.L.: Addition of ferromagnetic $CoFe_2O_4$ to YBCO thin films for enhanced flux pinning. Physica C **470**, S223 (2010). https://doi.org/10.1016/j.physc.2009.10.117
30. Sahoo, B., Behera, D.: Study of transport and elastic properties of YBCO superconductor by inclusion of GnPs. Phys. C Supercond. Its Appl. **578**, 1353748 (2020). https://doi.org/10.1016/j.physc.2020.1353748
31. Sumiya, H., Ishida, Y., Arimoto, K., Harano, K.: Real indentation hardness of nano-polycrystalline cBN synthesized by direct conversion sintering under HPHT. Diam. Relat. Mater. **48**, 47–51 (2014). https://doi.org/10.1016/j.diamond.2014.06.009
32. Asikuzun, E., Ozturk, O.: Theoretical and experimental comparison of micro-hardness and bulk modulus of orthorhombic $YBa_2Cu_{3-x}Zn_xO$ superconductor nanoparticles manufactured

using sol-gel method. Sak. Univ. J. Sci. **24**, 854–864 (2020). https://doi.org/10.16984/saufenbilder.676028
33. Asikuzun, E., Ozturk, O., Cetinkara, H.A., Yildirim, G., Varilci, A., Yilmazlar, M., Terzioglu, C.: Vickers hardness measurements and some physical properties of Pr_2O_3 doped Bi-2212 superconductors. J. Mater. Sci. Mater. Electron. **23**, 1001–1010 (2012). https://doi.org/10.1007/s10854-011-0537-0
34. Habanjar, K., Najem, A., Abdel-Gaber, A.M., Awad, R.: Effect of pelletization pressure on the physical and mechanical properties of (Bi, Pb)-2223 superconductors. Phys. Scr. **95**, 65702 (2020). https://doi.org/10.1088/1402-4896/ab7f46
35. Sangwal, K.: On the reverse indentation size effect and microhardness measurement of solids. Mater. Chem. Phys. **63**, 145–152 (2000). https://doi.org/10.1016/S0254-0584(99)00216-3
36. Awad, R., Abou Aly, A.I., Kamal, M., Anas, M.: Mechanical properties of (Cu0.5Tl0.5)-1223 substituted by Pr. J. Supercond. Nov. Magn. **24**, 1947–1956 (2011). https://doi.org/10.1007/s10948-011-1150-4
37. Feltham, P., Banerjee, R.: Theory and application of micro-indentation in studies of glide and cracking in single crystals of elemental and compound semiconductors. J. Mater. Sci. **27**(6), 1626–1632 (1992). https://doi.org/10.1007/BF00542926